⌘ *Author's Choice*

THE JOURNAL OF BIOLOGICAL CHEMISTRY VOL. 284, NO. 32, pp. 21536–21544, August 7, 2009

Functions of MutLα, Replication Protein A (RPA), and HMGB1 in 5′-Directed Mismatch Repair*[S]

Received for publication, May 14, 2009 Published, JBC Papers in Press, June 10, 2009, DOI 10.1074/jbc.M109.021287

Jochen Genschel[‡] **and Paul Modrich**[‡§1]

From the [‡]*Department of Biochemistry and the* [§]*Howard Hughes Medical Institute, Duke University Medical Center, Durham, North Carolina 27710*

A purified system comprised of MutSα, MutLα, exonuclease 1 (Exo1), and replication protein A (RPA) (in the absence or presence of HMGB1) supports 5′-directed mismatch-provoked excision that terminates after mismatch removal. MutLα is not essential for this reaction but enhances excision termination, although the basis of this effect has been uncertain. One model attributes the primary termination function in this system to RPA, with MutLα functioning in a secondary capacity by suppressing Exo1 hydrolysis of mismatch-free DNA (Genschel, J., and Modrich, P. (2003) *Mol. Cell* 12, 1077–1086). A second invokes MutLα as the primary effector of excision termination (Zhang, Y., Yuan, F., Presnell, S. R., Tian, K., Gao, Y., Tomkinson, A. E., Gu, L., and Li, G. M. (2005) *Cell* 122, 693–705). In the latter model, RPA provides a secondary termination function, but together with HMGB1, also participates in earlier steps of the reaction. To distinguish between these models, we have reanalyzed the functions of MutLα, RPA, and HMGB1 in 5′-directed mismatch-provoked excision using purified components as well as mammalian cell extracts. Analysis of extracts derived from A2780/AD cells, which are devoid of MutLα but nevertheless support 5′-directed mismatch repair, has demonstrated that 5′-directed excision terminates normally in the absence of MutLα. Experiments using purified components confirm a primary role for RPA in terminating excision by MutSα-activated Exo1 but are inconsistent with direct participation of MutLα in this process. While HMGB1 attenuates excision by activated Exo1, this effect is distinct from that mediated by RPA. Assay of extracts derived from *HMGB1*$^{+/+}$ and *HMGB1*$^{-/-}$ mouse embryo fibroblast cells indicates that HMGB1 is not essential for mismatch repair.

DNA mismatch repair provides several genetic stabilization functions but is best known for its role in the correction of replication errors (reviewed in Refs. 1–5). When triggered by a mismatched base pair, removal of a DNA biosynthetic error by this system is targeted to the newly synthesized strand by secondary signals within the helix. Although the strand signals that direct eukaryotic mismatch repair have not been identified, a strand break in the form of a nick or gap is sufficient to direct repair to the discontinuous strand in cell extracts, and there is evidence that similar signals may function *in vivo* (6). Analysis of the cell extract reaction has shown that the mammalian repair system possesses a bidirectional capability in the sense that the strand break that directs repair can be located either 3′ or 5′ to the mismatch (7–9).

Several purified mammalian systems have been described that support 3′ and/or 5′-directed mismatch-provoked excision or repair (10–13). The simplest of these depends on the mismatch recognition activities MutSα (MSH2·MSH6 heterodimer) or MutSβ (MSH2·MSH3 heterodimer), MutLα (MLH1·PMS2 heterodimer), the single-stranded DNA-binding protein replication protein A (RPA),[2] and the 5′ to 3′ double-strand hydrolytic activity Exo1 (exonuclease 1). These four activities support a mismatch-provoked excision reaction directed by a 5′ strand break, and excision terminates upon mismatch removal. MutLα is not essential for this excision reaction, but together with RPA has been implicated in excision termination (10, 12). In addition, the non-histone protein HMGB1 has been found to be required for mismatch repair in partially fractionated mammalian nuclear extracts (14). This small DNA binding protein has been postulated to functionally complement RPA in this 5′-directed system (12).

Supplementation of MutSα, MutLα, RPA, and Exo1 with the replication clamp PCNA proliferative cell nuclear antigen (PCNA) and the clamp loader replication factor C (RFC) yields a system that supports mismatch-provoked excision directed by a 3′ or 5′ strand break (11). The basis of the bidirectional excision capability of this system was clarified with the demonstration that MutLα is a latent endonuclease that is activated in a mismatch-, MutSα-, RFC-, and ATP-dependent fashion (15). Incision by activated MutLα is restricted to the discontinuous strand of a nicked heteroduplex and tends to occur on the distal side of the mismatch. Thus, for a nicked heteroduplex in which the strand break resides 3′ to the mismatch, activated MutLα introduces an additional strand break 5′ to the mispair. This 5′ strand discontinuity provides the loading site for the 5′ to 3′ excision system described above, which removes the mismatch.

MutSα has been shown to activate the 5′ to 3′ hydrolytic function of Exo1 on heteroduplex DNA, rendering the exonuclease highly processive, an effect attributed to physical interaction of the two activities (10). However, there are differences in the literature with respect to the roles of RPA and MutLα in

* This study was supported, in whole or in part, by National Institutes of Health Grant R01 GM45190 from the NIGMS.

⌘ *Author's Choice*—Final version full access.

[S] The on-line version of this article (available at http://www.jbc.org) contains supplemental Figs. S1 and S2.

[1] An Investigator of the Howard Hughes Medical Institute. To whom correspondence should be addressed. Tel.: 919-684-2775; Fax: 919-681-7874; E-mail: modrich@biochem.duke.edu.

[2] The abbreviations used are: RPA, replication protein A; BSA, bovine serum albumin; PCNA, proliferative cell nuclear antigen; MEF, mouse embryo fibroblast.

the control of this processive activity that leads to termination of 5′-directed excision (10, 12). One study has ascribed the primary excision termination function to RPA, which was shown to reduce the processive hydrolytic tracts of the MutSα·Exo1 complex from ≈2,000 to ≈250 nucleotides and by binding to gaps, to restrict Exo1 access to 5′ termini in excision intermediates and products (10). Analysis of excision intermediates as a function of nick-mismatch separation distance led to the conclusion that MutSα is able to reload Exo1 at an RPA-filled gap provided that a mismatch remains in the molecule; however, excision is attenuated upon mismatch removal because MutSα is no longer able to assist in this regard. In this mechanism MutLα functions in excision termination by suppressing nonspecific hydrolysis of the mismatch-free product, an effect attributed to its function as a general negative regulator of Exo1 (10, 16). By contrast, a second study has attributed the primary termination function in this 5′-directed excision system to MutLα, with RPA playing a secondary role (12). In this mechanism RPA has several proposed functions. It is postulated to bind to the 5′ strand break where MutSα recruits HMGB1. RPA and HGB1 then partially melt the helix in the vicinity of the strand break leading to recruitment of Exo1, which initiates processive 5′ to 3′ hydrolysis. Binding of RPA to the ensuing gap results in displacement of MutSα and HMGB1 from the DNA and promotes physical interaction of the exonuclease with MutLα. This results in Exo1 inactivation and dissociation of the MutLα·Exo1 complex from the substrate. As in the other mechanism described above, Exo1 is reloaded if a mismatch remains within the DNA.

To distinguish between these models, we have reassessed the roles of MutLα, RPA, and HMGB1 in mammalian mismatch repair. We demonstrate that 5′-directed excision terminates normally in extracts of A2780/AD cells, which support 5′-directed mismatch repair despite deficiency of MLH1 and PMS2 (17). Reanalysis of 5′-directed mismatch-provoked excision in the purified system described above has confirmed a direct role for RPA in terminating processive excision by MutSα-activated Exo1 but is inconsistent with direct participation of MutLα in this process. These experiments also indicate that while HMGB1 can attenuate Exo1 excision, this effect is distinct from that mediated by RPA. We also show that in contrast to results obtained with partially fractionated HeLa extracts (14), extracts derived from *HMGB1*$^{-/-}$ mouse embryo fibroblast cells are fully proficient in mismatch repair.

EXPERIMENTAL PROCEDURES

Cell Culture and Nuclear Extracts—Cell lines HeLa S3 and A2780/AD were grown and nuclear extracts prepared as described previously (7, 17). Nuclear extracts from these cell lines were concentrated by precipitation with 420 g/liter ammonium sulfate, dialyzed against 25 mM Hepes-KOH, pH 7.5, 100 mM KCl, 2 mM dithiothreitol, 0.1 mM EDTA, 0.1% (v/v) phenylmethylsulfonylfluoride (Sigma, relative to a saturated stock in isopropyl alcohol), 1 μg/ml leupeptin (Peptides International), 0.5 μg/ml E-64 (Peptides International), 0.1 μg/ml aprotinin (USB), quick-frozen in liquid nitrogen, and stored at −80 °C. Mouse embryonic fibroblast (MEF) cell lines VA-1 (*HMGB1*$^{+/+}$) and C-1 (*HMGB1*$^{-/-}$) (18), which were provided by Dr. Karen Vasquez (M. D. Anderson Cancer Center), were cultured as described (18, 19) and whole cell extracts prepared using published methods (20, 21). MEF extracts were frozen and stored as above.

Proteins—All proteins used in this study were ≥ 95% pure. MutSα was isolated from HeLa nuclear extract (22, 23). Human MutLα and Exo1 were prepared from recombinant baculovirus-infected insect cells as described (10, 23). Recombinant human RPA and His_6-tagged HMGB1 were prepared using *Escherichia coli* expression plasmids (24, 25), and RPA was isolated as described (10). His_6-tagged HMGB1 was prepared by a modification of the procedure of Yuan *et al.* (14). After chromatography on nickel-agarose (Qiagen), the eluate was adjusted to ~0.2 M NaCl and passed through a 1-ml MonoS column (HR 5/5, GE Healthcare) at 0.5 ml/min. His_6-HMGB1, which was present in the flow through, was further purified by chromatography on a 1-ml MonoQ column (HR 5/5, GE Healthcare) (14). Electrospray mass spectroscopy confirmed the full-length nature of purified His_6-HMGB1. Protein concentrations were determined by Bradford assay using bovine serum albumin (BSA) as standard.

DNA Substrates—6,440 bp 5′ G-T heteroduplex DNAs were constructed using bacteriophages f1MR1 and f1MR3 (26) and contained a strand-specific single-strand break 128, 494, or 808 bp 5′ to the mismatch as viewed along the shorter path in the circular molecules (9). A G-T heteroduplex containing a strand break 128 bp 3′ to the mismatch was prepared in a similar manner using phages f1MR70 and f1MR71, which were constructed by oligonucleotide mutagenesis of f1MR1 and f1MR3, respectively. Mutagenesis substituted an EcoRV sequence for residues 5501–5506 of these two phage DNAs. Circular f1MR1 homoduplex DNA containing a 314-nucleotide gap in the complementary DNA strand between the AccI and HincII sites was prepared as described (10).

Mismatch Repair Activity Assays—Mismatch repair in MEF whole cell extracts was determined by restriction site restoration assay as described previously (7, 23). Briefly, reactions (20 μl) contained 100 μg of MEF extract, 5′ or 3′ G-T heteroduplex (100 ng, 24 fmol, nick-mismatch separation distance of 128 bp), 20 mM Tris-HCl, pH 7.6, 5 mM $MgCl_2$, 100 mM KCl, 1.5 mM ATP, 0.1 mM (each) dNTPs, 1 mM glutathione, and 50 μg/ml BSA. When indicated, reactions were supplemented with 100 ng (3.3 pmol) of recombinant HMGB1 (HMGB1 and all other purified used in this study were diluted as necessary into 7.5 mM HEPES-KOH pH 7.5, 200 mM KCl, 0.6 mM dithiothreitol, 2 mg/ml BSA, 10% (v/v) glycerol). After deproteinization and cleavage with HindIII and ClaI, repair products were resolved by agarose gel electrophoresis and quantified after ethidium staining with a cooled photometric grade CCD imager (Photometrics Inc.).

5′-Directed mismatch-provoked excision in cell-free extract was performed in a similar manner except that dNTPs were omitted and A2780/AD nuclear extract (supplemented as indicated with recombinant MutLα) was used. Reactions were scaled up to monitor the reaction time course (50 μg of A2780/AD nuclear extract, 24 fmol of heteroduplex, and MutLα as indicated per 20-μl time sample). The DNA substrate was preincubated in the absence or presence of MutLα for 5

min at 37 °C, and the reaction initiated by extract addition. Mismatch-provoked excision in a purified system was performed in the absence of dNTPs as described previously (10) in reactions (20 μl of final volume per time sample) that contained 100 ng of 5′ G-T heteroduplex (24 fmol, nick-mismatch separation distance as specified), 100 ng of MutSα (400 fmol), and as indicated 100 ng of RPA (900 fmol), 50–200 ng of MutLα (280–1100 fmol), and 100 ng of HMGB1 (3.3 pmol). After incubation at 37 °C for 5 min, hydrolysis was initiated by addition of 2 ng of Exo1 (21 fmol).

Two assays were used to score excision that occurred in these reactions. In one method, DNA recovered from an excision reaction (27) was digested with NheI and ClaI (2 units each) and digestion products quantified after agarose gel electrophoresis and ethidium staining as described above. As illustrated in Fig. 1, this assay scores conversion of an NheI site located 5 bp from the mismatch to an endonuclease-resistant form (23). The second method is based on localization of excision tract end points by indirect end-labeling (9, 23). In these experiments, DNA isolated from reactions using purified proteins was digested with AseI (5 units) or ClaI (2 units). For assays performed using nuclear extracts and the G-T heteroduplex with a 128-bp mismatch strand break separation distance, reaction products were digested with AseI (5 units) and Sau96I (0.5 units). Double digestion in this manner restores the original strand break in the substrate, which is subject to partial ligation in extracts (9). Restriction products were resolved by electrophoresis through 2% (AseI digests) or 1% (ClaI digests) alkaline-agarose. DNA was transferred to nylon membranes (Hybond XL, GE Healthcare), which were probed with ^{32}P-labeled oligonucleotides that hybridize to the complementary DNA strand adjacent to the AseI or ClaI site. These probe sequences correspond to f1MRviral strand nucleotides 4634–4653 (d(AACGTTCGGGCAAAGGATTT); probe V4634 for AseI digests) or 2532–2552 (d(TGGTTTCATTGGTGACGTTTC); probe V2532 for ClaI digests) (26).

Western Blots—Polyacrylamide gel electrophoresis and transfer to polyvinylidene difluoride membranes was performed as described previously (28). Antibodies used were rabbit anti-MLH1 (AB-2, EMD Biosciences), rabbit anti-MSH6 (28), and rabbit anti-HMGB1 (BD Pharmingen). Staining for loading controls was done with Ponceau S (Sigma).

RESULTS

5′-Directed Excision in MutLα-deficient A2780/AD Nuclear Extracts—Several drug-resistant derivatives of A2780 ovarian tumor cells have been shown to be deficient in 3′- but not 5′-directed mismatch repair and to be devoid of detectable MLH1 (17, 29), defects that have generally been attributed to silencing of MLH1 expression (30). Because extracts derived from adriamycin-resistant A2780/AD cells lack MLH1 but nevertheless support robust 5′-directed mismatch repair (17), we have utilized this system to evaluate the role(s) of MutLα in termination of 5′-directed excision. The MLH1 deficiency of this cell line is reversed upon treatment with 2′-deoxy-5-azacytidine,[3] suggesting that its orientation-dependent repair defect is also due to *MLH1* silencing.

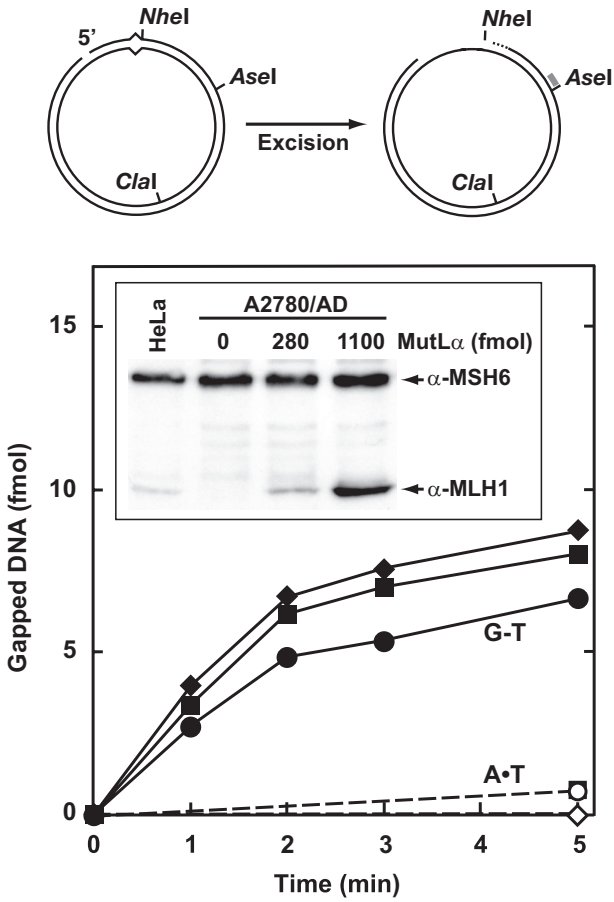

FIGURE 1. **Mismatch-provoked excision in A2780/AD nuclear extracts.** The *upper diagram* illustrates the nature of the substrates and excision assays used in this study. 6.44 kb circular heteroplexes contained a G-T mismatch (A·T base pair in homoduplex controls) and a site-specific strand break, which was located 5′ to the mismatch as viewed along the shorter path between the two sites. Although DNAs used contain 4 AseI sites, only the site proximal to the mismatch shown in the diagram was used in this work. Two methods were used to score excision products. A single NheI site, separated from the mismatch by 5 base pairs, is rendered endonuclease-resistant by mismatch-provoked excision, an effect that was monitored by digestion of reaction products with NheI and ClaI (23). In the second method, 5′-termini produced by excision were localized by digestion with AseI, resolved by electrophoresis through alkaline-agarose gels, and products probed by indirect end-labeling using a ^{32}P-labeled oligonucleotide that hybridizes to the processed strand adjacent to the AseI site (*gray bar* in *right diagram*). *Lower*, NheI resistance assay was used to score 5′-directed excision in nuclear extracts of A2780/AD cells, which are deficient in MLH1 and PMS2 (17). Excision reactions contained 5′ G-T heteroduplex (*closed symbols*, nick 128 bp 5′ to mismatch) or otherwise identical A·T homoduplex control DNA (*open symbols*), 50 μg of nuclear extract without (*circles*), or supplemented with 280 fmol (*squares*) or 1100 fmol (*diamonds*) MutLα. The *inset* shows a Western blot for MSH6 and MLH1 in 50 μg of nuclear extract derived from HeLa or A2780/AD cells, in the latter case in the absence of MutLα or supplemented with 280 or 1100 fmol of the repair protein.

As shown in Fig. 1, nuclear extracts derived from A2780/AD cells support efficient excision on a 5′ heteroduplex, an effect that depends on the presence of a mismatched base pair. Supplementation of these extracts with recombinant MutLα to a level comparable to that present in HeLa cell nuclear extract (Fig. 1, *inset*), resulted in about 25% enhancement of 5′-directed excision, but higher levels of the repair protein provided no significant additional stimulation. Previous studies have shown

[3] R. Brown, personal communication.

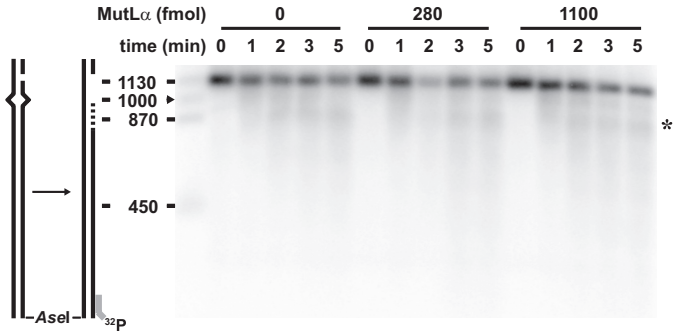

FIGURE 2. **Excision termination in A2780/AD nuclear extracts.** Mismatch-provoked excision reactions ("Experimental Procedures") contained 5′ G-T heteroduplex DNA (128-bp nick-mismatch separation distance) and 50 μg of A2780/AD nuclear extract supplemented as indicated with MutLα. After digestion with AseI and Sau96I, products were subjected to electrophoresis through alkaline-agarose, transferred to a nylon membrane, and probed with ^{32}P-labeled oligonucleotide V4634, which hybridizes to the discontinuous heteroduplex strand adjacent to the AseI site (see diagram on *left* and Fig. 1). The major zone of termination products (*asterisk*) peaks at about 870 nucleotides (the AseI cleavage site is 1,000 bp from the mismatch). A tail of smaller material extending in size down to about 350 nucleotides is also evident, particularly at longer incubation times, and this material is potentiated by the presence of MutLα.

that while MutLα supplementation of A2780/AD extracts alleviates the defect in 3′-directed mismatch repair, the protein only modestly stimulates the already near normal level of 5′-directed repair characteristic of this cell line (17). The modest enhancement described here for 5′-directed mismatch-provoked excision is consistent with these previous findings. Results obtained with A2780/AD extracts are also consistent with the MutLα independence of 5′-directed excision and repair that has been observed in several purified systems (10–13).

Indirect end-labeling (9) was used to map excision termination endpoints produced in A2780/AD extract. As shown in the first six lanes of Fig. 2, excision is time-dependent with the major termination zone (*asterisk*) centered 130–140 nucleotides beyond the mispair. In addition, some smaller material indicative of excision tracts extending as much as 600 nucleotides beyond the mismatch was also evident, particularly at longer incubation times. MutLα supplementation did not significantly alter excision kinetics or the location of the major termination zone (Fig. 2, *lanes 6–15*). However, the presence of the repair protein did enhance the production of smaller material, an effect that may be due to MutSα-, RFC-, and PCNA-dependent activation of the MutLα endonuclease, which can incise the discontinuous strand of a nicked circular heteroduplex at substantial distances from the mispair (15). These findings indicate that MutLα is not essential for excision termination in nuclear extracts.

Termination events in A2780/AD extracts are similar to those previously described in extracts of MutLα-proficient HeLa cells (9). To determine whether the region in which termination occurs depends on nick-mismatch separation distance, we repeated the HeLa nuclear extract excision studies using three 5′ heteroduplexes, in which the location of the G-T mismatch was constant but location of the 5′ strand break was varied (supplemental Fig. S1). Although the efficiency with which excision tracts reached the mispair decreased with increasing separation distance (128, 494, or 808 bp), the primary termination zone with all three heteroduplexes was centered 130–140 nucleotides beyond the mismatch. As observed in A2780/AD extracts, this major termination zone was accompanied by production of smaller material corresponding to the 5′-termini located as much as 600 nucleotides beyond the mismatch.

MutLα Effects on 5′-Directed Excision in a Purified System—A purified system comprised of MutSα, MutLα, RPA, Exo1, and HMGB1 supports 5′-directed mismatch-provoked excision (10, 12). The concentrations of the protein components used in this system are similar to those present in 50–100 μg of nuclear extract, extract levels routinely used to study cell-free mismatch repair. Efficient excision in this system depends strongly on Exo1, MutSα, and RPA. HMGB1 can partially substitute for RPA in the reconstituted reaction, but MutLα is not required for mismatch-provoked hydrolysis. As discussed above, previous work with this model system has led to the suggestion that together with RPA, MutLα functions in excision termination. One study has attributed the primary termination function to RPA, with MutLα acting after the fact to stabilize excision products by suppressing Exo1 hydrolysis of the now mismatch-free DNA, an effect that also enhances the mismatch dependence of the reaction (10). A second study ascribes to MutLα an active role as the primary factor that terminates excision by MutSα-activated Exo1 (12).

To distinguish these possibilities, we have evaluated the kinetics of heteroduplex hydrolysis supported by MutSα, Exo1, and RPA as a function of nick-mismatch separation distance (128, 494, or 808 bp), and the absence or presence of MutLα. Previous experiments have demonstrated that 280 fmol of MutLα (~3 times that present in 50 μg of HeLa nuclear extract; see Fig. 1, *inset*) is optimal for 5′-directed excision in the purified system used here. Two major zones of excision termination were observed with all heteroduplexes, corresponding to progression of hydrolysis to about 40–100 or 220–350 nucleotides beyond the mismatch (Fig. 3). These species were observed in the absence or presence of 280 fmol of MutLα, indicating that MutLα is not required for their production. Both species were metastable and subject to additional hydrolysis, particularly at long incubation times in the absence of MutLα. Supplementation of the reactions with 280 fmol of the MHL1·PMS2 heterodimer increased the lifetime of both species, rendering them less susceptible to further hydrolysis, an effect that is particularly apparent for the heteroduplexes in which the nick and mismatch are separated by 128 or 494 bp (Fig. 3).

Because some experiments with this reconstituted 5′-excision system have utilized as much as 1100 fmol of MutLα (12), about 12 times that present in 50 μg of nuclear extract, we have also evaluated effects of high levels of the protein on excision with the three heteroduplexes. As can be seen in Fig. 3, the primary excision product produced in the presence of 1100 fmol of MutLα corresponds to the species located 40–100 nucleotides beyond the mismatch, with only low levels of the smaller product observed. However, this is accompanied by a general inhibition of mismatch-provoked hydrolysis, an effect that is particularly evident in the accumulation of excision intermediates that fail to reach the mismatch within the incu-

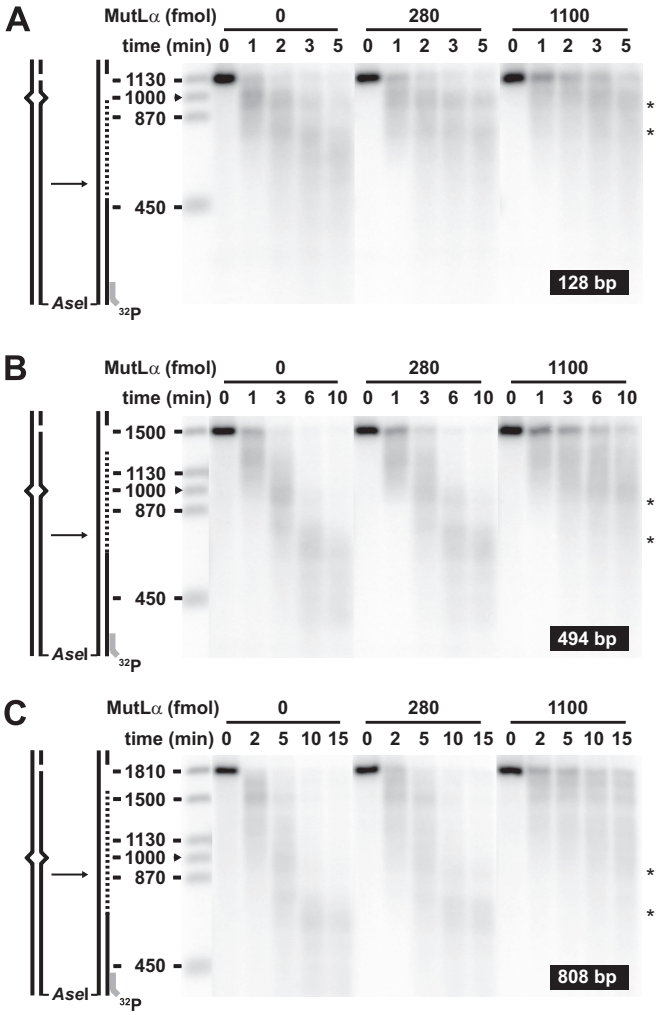

FIGURE 3. **Effects of MutLα on 5′-directed excision in a purified system.** Excision reactions ("Experimental Procedures") contained per time sample 24 fmol of 5′ G-T heteroduplex DNA, 400 fmol of MutSα, 900 fmol of RPA, 21 fmol of Exo1, and MutLα as indicated. Excision was visualized by hybridization assay (probe V4634) after AseI digestion and alkaline electrophoresis through 2% agarose ("Experimental Procedures") as illustrated in the diagrams on the *left*. Separation distances between the nick and the mismatch were 128 (*A*), 494 (*B*), or 808 bp (*C*). Two major termination zones were observed with each DNA (*asterisks*). As discussed in the text, stability of these zones was modulated by the presence of MutLα.

bation times employed (Fig. 3). Taken together, these findings indicate that MutLα does not play an active role in excision termination in this system, but rather functions to stabilize excision products produced during the course of the MutSα-, Exo1-, and RPA-dependent reaction.

MutLα and MutSα have previously been shown to suppress Exo1 hydrolysis of DNA that lacks a mismatch (10, 16). For purposes of comparison with the heteroduplex results described above, we have used the indirect end-labeling assay employed in Figs. 2 and 3 to monitor the effect of MutLα on Exo1 hydrolysis of nicked homoduplex DNA in the presence of MutSα and RPA (Fig. 4). Results with the mismatch-free DNA differ dramatically from those obtained with heteroduplex substrates. As can be seen, incubation with MutSα, RPA, and Exo1 resulted in very slow 5′ to 3′ hydrolysis from the strand break at an average rate of about 10 nucleotides min^{-1}. Furthermore, digestion in this manner was largely suppressed by the presence

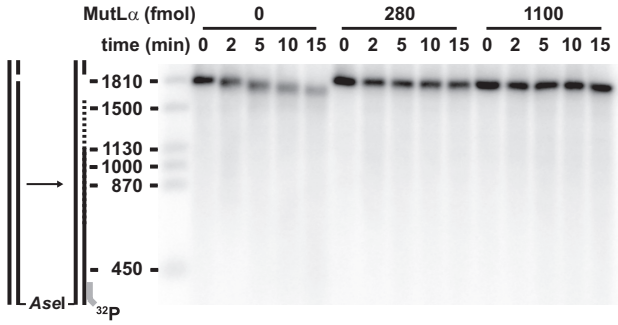

FIGURE 4. **Excision on homoduplex DNA in the purified system.** Excision reactions were performed as described in the legend to Fig. 3*C* except that the substrate contained an A·T base pair instead of a G-T mismatch.

of MutLα, with 280 fmol of the protein being largely sufficient in this regard. These results confirm previous conclusions concerning the negative regulatory effect of MutLα on Exo1 hydrolysis of homoduplex DNA and substantiate the idea that the role of this activity in terminating Exo1 hydrolysis is the stabilization of primary excision products.

HMGB1 Effects on 5′-Directed Excision in the Purified System—The nonhistone chromatin protein HMGB1 interacts with MutSα (14) and has been postulated to provide an RPA-like function in the reconstituted 5′-directed excision system (12). To evaluate this idea, excision was scored with the heteroduplex set described above in reactions containing MutSα, Exo1, and MutLα in the absence or presence of HMGB1 or HMHB1 plus RPA (Fig. 5; hydrolysis supported by MutSα, Exo1, and MutLα under these conditions, but in the presence of RPA only is shown in the central panels of Fig. 3). Heteroduplex excision was limited in the absence of the two DNA-binding proteins (Fig. 5, *right panels*). The hydrolytic products that are visible only during the first minute or two in the right panels of Fig. 5 are produced by highly processive digestion of a small subset of molecules (10), an effect that will be considered further below.

As can be seen from the levels of undigested material and in agreement with previous findings (10, 12), supplementation with RPA (Fig. 3, *center panels*) or HMGB1 (Fig. 5, *center panels*) activated heteroduplex hydrolysis in this system, with RPA being much more effective in this regard. Supplementation with both RPA and HMGB1 resulted in hydrolytic patterns similar, but not identical to those observed with RPA alone. The presence of HMGB1 kinetically stabilized the primary termination products produced in the presence of MutSα, MutLα, Exo1, and RPA (compare Fig. 5, *left panels* with Fig. 3, *center panels*), an effect that is particularly apparent for the heteroduplexes in which the nick-mismatch separation distance was 128 or 494 bp. However, it can also be seen that HMGB1 supplementation of MutSα, MutLα, Exo1, and RPA resulted in a general inhibition of hydrolysis. In the case of the G-T heteroduplex with an 808-bp nick-mismatch separation distance, the consequence of this effect was failure of a substantial fraction of the excision tracts to reach the mismatch within the 15-min time course of the experiment. Thus, as in the case of MutLα, the primary effect of HMGB1 on excision in this system appears to be the stabilization of primary termination products that are produced naturally as a consequence of hydrolysis by MutSα-activated Exo1 in the presence of RPA.

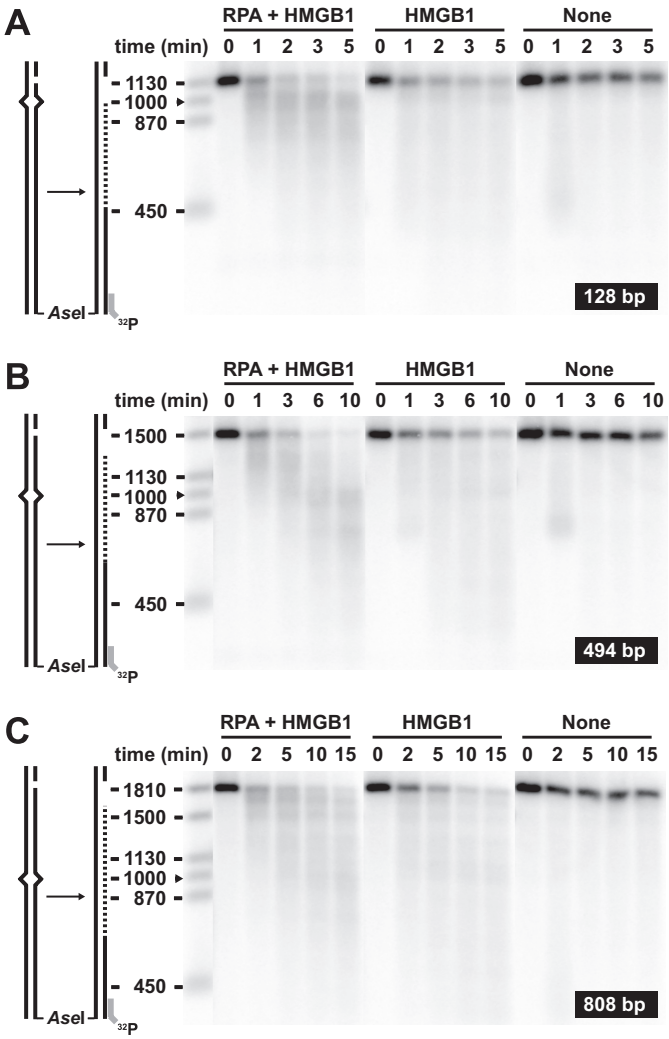

FIGURE 5. **HMGB1 effects on excision tracts in the purified system.** Mismatch-provoked excision reactions, performed and analyzed as in Fig. 3, contained per time sample 400 fmol of MutSα, 21 fmol of Exo1, 280 fmol of MutLα, and as indicated, 900 fmol of RPA, 3.3 pmol of HMGB1, or neither RPA or HMGB1. G-T heteroduplexes contained a strand break located 128 (*A*), 494 (*B*), or 808 bp (*C*) 5′ to the mispair.

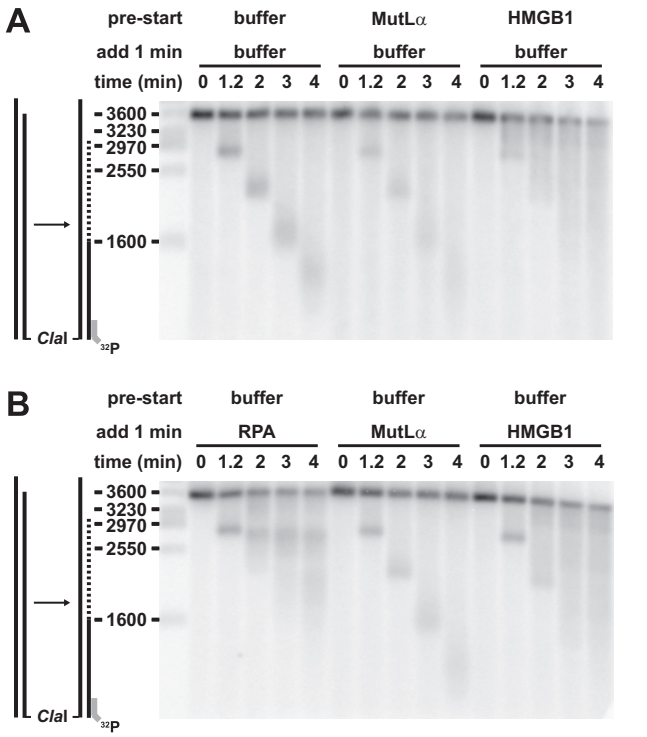

FIGURE 6. **Effects of RPA, MutLα, and HMGB1 on the processive action of MutSα-activated Exo1.** Protein challenge was used to evaluate effects of repair activities on processive hydrolysis by activated Exo1. *A*, reactions contained (per time sample) 24 fmol of gapped homoduplex DNA substrate (gap size 314 nucleotides) and 400 fmol of MutSα. After 5 min at 37 °C, hydrolysis was initiated at time 0 by addition of 21 fmol of Exo1 in the absence (buffer, *left*) or presence of either 280 fmol of MutLα (*middle*) or 3.3 pmol of HMGB1 (*right*). Reaction conditions were the same as those used for mismatch-provoked excision ("Experimental Procedures") except that the volume per time sample was reduced to 18.4 μl to accommodate the further addition at 1 min of 1.6 μl buffer (16 mM HEPES-KOH pH 7.5, 100 mM KCl, 0.3 mM dithiothreitol, 1 mg/ml BSA, 5% (v/v) glycerol). Reactions were sampled (20 μl), hydrolysis quenched, and products visualized after cleavage with ClaI, alkaline-agarose gel electrophoresis, Southern transfer, and hybridization with probe V2532 ("Experimental Procedures"). *B*, reaction conditions were as in *panel A*, except that hydrolysis was initiated by addition of Exo1 only. At 1 min, reactions were supplemented per time sample with 900 fmol of RPA (*left*), 280 fmol of MutLα (*middle*), or 3.3 pmol of HMGB1 (*right*) in 1.6 μl of buffer.

Termination of Hydrolysis by MutSα-activated Exo1 Is Independent of MutLα or HMGB1—We have previously shown that MutSα activates Exo1 on gapped homoduplex DNA to form a highly processive hydrolytic complex that is regulated by RPA (10). In such experiments, circular homoduplex DNA containing a 314-nucleotide gap is preincubated with MutSα, excision initiated by addition of Exo1, and effects of other repair proteins on the reaction determined as a function of their presence during pre- or post-initiation stages of hydrolysis. The regulatory effects of RPA on the MutSα·Exo1 complex are illustrated in Fig. 6. In the absence of other proteins, MutSα-activated Exo1 hydrolyzes a subset of the gapped substrate molecules at a constant rate of about 580 nucleotides min^{-1} (Fig. 6*A*, *left panel*), a manifestation of its processive nature, leading to removal of about 2,000 nucleotides prior to dissociation (10). However, and as observed previously (10), if RPA is added after initiation of hydrolysis, then digestion continues for about 200 nucleotides at which point it is dramatically attenuated (Fig. 6*B*, *left*).

We have used this procedure to evaluate the effects of MutLα and HMGB1 on the hydrolytic properties of MutSα-activated Exo1. Inclusion of MutLα during the preincubation stage of the assay reduced the fraction of substrate susceptible to digestion, but the presence of MutLα was without effect on progression of the processive events that did initiate under these conditions (Fig. 6*A*, *center*). Similarly, post-initiation addition of the MLH1·PMS2 heterodimer had no significant effect on the progression of ongoing processive hydrolytic events (Fig. 6*B*, *center*). RPA effects were also evaluated in reactions in which MutLα was present during the preincubation stage. As observed in the absence of MutLα, postinitiation addition of RPA resulted in arrest of hydrolysis after removal of about 200 additional nucleotides (supplemental Fig. S2*B*, *left*), whereas inclusion of the DNA-binding protein during the preincubation stage led to a general attenuation of excision (supplemental Fig. S2*A*, *left*), an effect similar to that observed previously in reactions lacking MutLα (10).

Effects of HMGB1 in this system were different from those of RPA or MutLα. Inclusion of HMGB1 during the pre-incubation

stage of the reaction generally inhibited formation of the processive complex as judged by failure to produce the pseudo-discrete hydrolytic species characteristic of this complex (compare *left* and *right panels* of Fig. 6*A*). However, hydrolysis did occur under these conditions resulting in relatively continuous product distribution spanning a size range of several thousand nucleotides. When HMGB1 was added to reactions in which processive hydrolysis was ongoing, further processive digestion was significantly inhibited, but in a manner much less dramatic than the termination effects observed with RPA (compare *left* and *right panels* of Fig. 6*B*). Similar effects of HMGB1 were also observed in reactions in which both MutLα and MutSα were present during the preincubation stage (supplemental Fig. S2, *center panels*). The distribution of hydrolytic products observed in reactions supplemented with both RPA and HMGB1, either during preincubation or after Exo1 addition, was similar to those obtained with RPA alone (supplemental Fig. S2); however, the presence of HMGB1 significantly potentiated RPA suppression of Exo1 hydrolysis, particularly in the case where both proteins were present during the preincubation stage of the reaction.

HMGB1 Is Dispensable for Mismatch Repair in Mouse Cell Extracts—The initial conclusion that HMGB1 is required for mammalian mismatch repair was based on several observations (14): (i) partially fractionated HeLa nuclear extract, which would not support mismatch repair, would do so when supplemented with RPA and HMGB1; (ii) immunodepletion of HMGB1 reduced the efficiency of mismatch repair in HeLa extract by about 60%; and (iii) MSH2 was shown to co-immunoprecipitate with HMGB1 in a purified system. To directly evaluate the requirement for HMGB1 in an unfractionated extract system, we have exploited the availability of the MEF cell line that harbors a complete deletion of the *HMGB1* locus (18, 19). As shown in Fig. 7, extracts of *HMGB1*$^{-/-}$ MEF cells support robust mismatch repair directed by a strand break located either 3′ or 5′ to the mismatch. Furthermore, supplementation of extracts derived from either *HMGB1*$^{-/-}$ or *HMGB1*$^{+/+}$ cells with near homogeneous recombinant human HMGB1 did not significantly affect repair efficiencies in either case. Possible explanations for these different findings will be considered below.

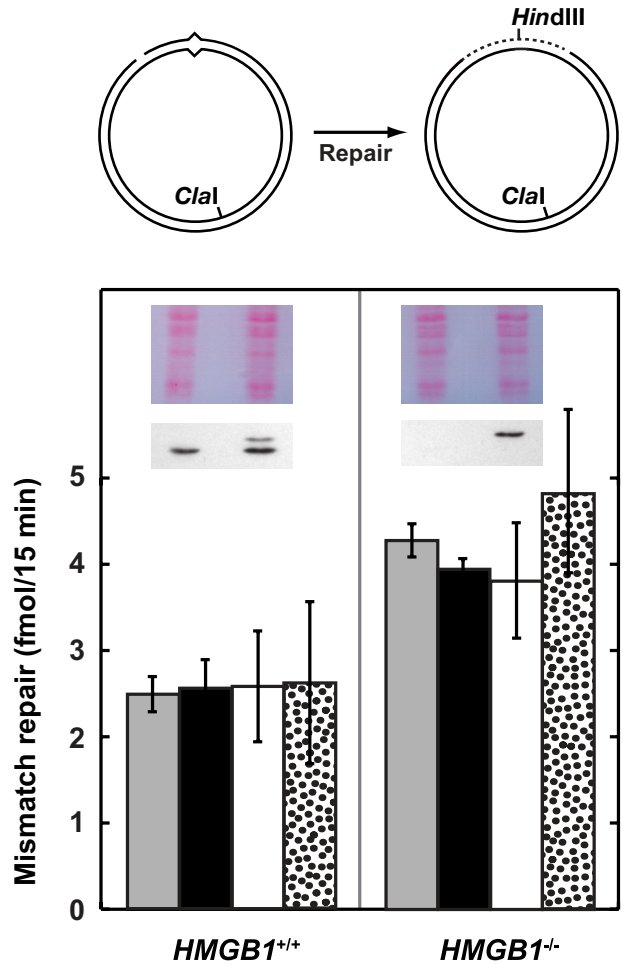

FIGURE 7. **Mismatch repair in HMGB1-deficient MEF cell extracts.** Mismatch repair of 5′ (*gray* and *black bars*) or 3′ (*white* and *stippled bars*) G-T heteroduplexes in HMGB1-proficient or -deficient MEF cell extracts was determined in the absence (*gray* and *white bars*) or presence (*black* and *stippled bars*) of 3.3 pmol of recombinant HMGB1 as described under "Experimental Procedures." Heteroduplex orientation refers to the 3′ or 5′ location of the strand break relative to the mispair as viewed along the shorter path linking the two sites in the circular substrates used. As indicated in the *upper diagram*, repair was scored by restoration of HindIII sensitivity (26) as judged by cleavage with HindIII and ClaI. Reactions were done in triplicate, and error bars indicate 1 S.D. *Insets* show the results of HMGB1 Western blots obtained with 100 μg of HMGB1-proficient (*left*) or -deficient (*right*) extract unsupplemented (*left lanes* of each gel) or supplemented (*right lanes*) with 100 ng of recombinant human HMGB1. Because of the presence of a His_6 tag, the recombinant protein runs slower than endogenous HMGB1. Ponceau S staining of the Western membrane was used as a loading control.

DISCUSSION

Several drug-resistant human cell lines, in which the *MLH1* loci are silenced (30),[3] have been shown to be defective in 3′- but not 5′-directed mismatch rectification (17). We have shown here that extracts derived from one of these cell lines, A2780/AD, supports mismatch-dependent 5′-directed excision, proving that the 5′-directed rectification that was previously documented with this line is mismatch-provoked and hence corresponds to *bona fide* mismatch repair. As observed previously with respect to repair (17), we have also found that MutLα supplementation modestly enhances 5′-directed excision in these extracts, suggesting the potential existence of MutLα-dependent and -independent modes of 5′-directed excision in mammalian cells. Interestingly, previous studies have documented two distinct modes of 5′-directed excision in HeLa nuclear extracts with respect to PCNA involvement. While essentially all 3′-directed excision events that occur in HeLa extracts are PCNA-dependent, both PCNA-dependent and -independent modes of 5′-directed excision have been documented in this system (supplemental data in Refs. 10, 31).

We have also found that 5′-directed excision tracts that occur A2780/AD extracts terminate within the same region as do those that occur in extracts derived from MutLα-proficient HeLa cells (Figs. 2 and supplemental S1). Thus, the postulated requirement for MutLα in the termination of mismatch-provoked excision (12) can be ruled out for the extract system. Analysis of MutLα effects on the termination of hydrolysis by MutSα-activated Exo1 in a purified system is also consistent with this view. We have demonstrated previously in the presence of MutLα (10) and confirm here in the absence or presence

of MutLα, the dramatic effects of RPA on mismatch-provoked excision by MutSα-activated Exo1. Surprisingly, RPA has both positive and negative effector roles in this reaction. The single-strand-binding protein not only stimulates substrate turnover but also functions to stabilize reaction products after mismatch removal (compare *right panels* of Fig. 5 with the *center panels* of Fig. 3). Furthermore, the reaction products produced in the presence of RPA and MutLα are similar to those produced in the presence of RPA alone, although it is clear that MutLα does enhance their lifetime (compare *right* and *center panels* of Fig. 3). This substantiates the previous conclusion (10) that RPA functions as the primary termination activity in this system, with MutLα functioning after the fact to stabilize primary hydrolytic products against further Exo1 degradation.

We have also confirmed here the previous finding that RPA functions as a negative regulator of the MutSα·Exo1 complex, reducing its processivity from about 2,000 to about 200 nucleotides (Figs. 6 and supplemental S2). By contrast, MutLα is without significant effect on the processive behavior of activated Exo1. As described previously (10), we attribute the activating effect of RPA on mismatch-provoked excision to its ability to regulate processive behavior of the MutSa·Exo1 complex. In particular, we suggest that RPA-mediated displacement of MutSα and/or Exo1 excision intermediates and products permits the system to turn over.

We have also confirmed the ability of the nonhistone protein HMGB1 to stimulate excision by MutSα-activated Exo1 and have evaluated its effects on the processive behavior of this complex. In both cases HMGB1 behaved in a manner distinct from RPA. In amounts comparable to that present in 100 μg of nuclear extract (≈120 ng as judged by quantitative Western blot, data not shown), HMGB1 significantly stimulated mismatch-provoked excision (compare *center* and *right panels* of Fig. 5), but less effectively than RPA. As in the case of RPA, this effect may be due to the ability of HMGB1 to interfere with progression of the processive hydrolysis, forcing turnover of the hydrolytic complex. However, as can be seen in Fig. 6, HMGB1 was less effective than RPA with respect to its ability to disrupt processive excision.

As noted above, the most compelling evidence for an HMGB1 requirement in mammalian mismatch repair has derived from analysis of partially fractionated HeLa cell extracts, a system in which repair was shown to be strongly dependent on HMGB1 addition (14). Inasmuch as HMGB1-proficient and -null cell lines are available (18, 19), we have evaluated the mismatch repair requirement for this protein in whole cell extracts. In contrast to results obtained with partially fractionated extracts, we have found that unfractionated HMGB1-deficient extracts support robust mismatch repair that can be directed by either a 3′ or 5′ strand break. There are several possible explanations for these different findings. For example, mammalian cell extracts may possess a second activity, which provides a mismatch repair function that is redundant with respect to HMGB1; in this case, the fractionation method employed by Yuan *et al.* (14) may have resolved these two activities. An alternate possibility is that the fractionation method employed by Yuan *et al.* enriched for an inhibitor of the reaction, the action of which is reversed by HMGB1. Distinction between these and other possibilities must await further studies, but we note that as in the case of the unfractionated extracts used here, several purified systems have been described that support highly efficient mismatch repair in the absence of HMGB1 (12, 13).

Comparison of results obtained with the extract and purified systems described here has revealed significant differences in termination zones in the two cases. Excision occurring in extracts is characterized with a single primary termination zone centered about 130–140 nucleotides beyond the mispair. By contrast, two major termination zones occur in the purified system, located about 40–100 nucleotides or 220–350 nucleotides beyond the mismatch, with the former appearing to be a precursor to the latter. As described previously, we regard the reconstituted mismatch repair systems that have been described to date as minimal systems (4) and attribute the sort of difference noted above to as yet unidentified extract components that significantly modulate various steps of the reaction.

Acknowledgments—We thank K. Vasquez and M. Bianchi for the generous gift of HMGB1$^{+/+}$ and HMGB1$^{-/-}$ mouse embryonic fibroblast cell lines.

REFERENCES

1. Kunkel, T. A., and Erie, D. A. (2005) *Annu. Rev. Biochem.* **74,** 681–710
2. Iyer, R. R., Pluciennik, A., Burdett, V., and Modrich, P. L. (2006) *Chem. Rev.* **106,** 302–323
3. Jiricny, J. (2006) *Nat. Rev. Mol. Cell Biol.* **7,** 335–346
4. Modrich, P. (2006) *J. Biol. Chem.* **281,** 30305–30309
5. Li, G. M. (2008) *Cell Res.* **18,** 85–98
6. Pavlov, Y. I., Newlon, C. S., and Kunkel, T. A. (2002) *Mol. Cell* **10,** 207–213
7. Holmes, J., Jr., Clark, S., and Modrich, P. (1990) *Proc. Natl. Acad. Sci. U.S.A.* **87,** 5837–5841
8. Thomas, D. C., Roberts, J. D., and Kunkel, T. A. (1991) *J. Biol. Chem.* **266,** 3744–3751
9. Fang, W. H., and Modrich, P. (1993) *J. Biol. Chem.* **268,** 11838–11844
10. Genschel, J., and Modrich, P. (2003) *Mol. Cell* **12,** 1077–1086
11. Dzantiev, L., Constantin, N., Genschel, J., Iyer, R. R., Burgers, P. M., and Modrich, P. (2004) *Mol. Cell* **15,** 31–41
12. Zhang, Y., Yuan, F., Presnell, S. R., Tian, K., Gao, Y., Tomkinson, A. E., Gu, L., and Li, G. M. (2005) *Cell* **122,** 693–705
13. Constantin, N., Dzantiev, L., Kadyrov, F. A., and Modrich, P. (2005) *J. Biol. Chem.* **280,** 39752–39761
14. Yuan, F., Gu, L., Guo, S., Wang, C., and Li, G. M. (2004) *J. Biol. Chem.* **279,** 20935–20940
15. Kadyrov, F. A., Dzantiev, L., Constantin, N., and Modrich, P. (2006) *Cell* **126,** 297–308
16. Nielsen, F. C., Jäger, A. C., Lützen, A., Bundgaard, J. R., and Rasmussen, L. J. (2004) *Oncogene* **23,** 1457–1468
17. Drummond, J. T., Anthoney, A., Brown, R., and Modrich, P. (1996) *J. Biol. Chem.* **271,** 19645–19648
18. Calogero, S., Grassi, F., Aguzzi, A., Voigtländer, T., Ferrier, P., Ferrari, S., and Bianchi, M. E. (1999) *Nat. Genet.* **22,** 276–280
19. Lange, S. S., Mitchell, D. L., and Vasquez, K. M. (2008) *Proc. Natl. Acad. Sci. U.S.A.* **105,** 10320–10325
20. Challberg, M. D., and Kelly, T. J., Jr. (1979) *Proc. Natl. Acad. Sci. U.S.A.* **76,** 655–659
21. Tomer, G., Buermeyer, A. B., Nguyen, M. M., and Liskay, R. M. (2002) *J. Biol. Chem.* **277,** 21801–21809
22. Drummond, J. T., Li, G. M., Longley, M. J., and Modrich, P. (1995) *Science* **268,** 1909–1912
23. Genschel, J., Bazemore, L. R., and Modrich, P. (2002) *J. Biol. Chem.* **277,** 13302–13311

24. Henricksen, L. A., Umbricht, C. B., and Wold, M. S. (1994) *J. Biol. Chem.* **269,** 11121–11132
25. McKinney, K., and Prives, C. (2002) *Mol. Cell. Biol.* **22,** 6797–6808
26. Su, S. S., Lahue, R. S., Au, K. G., and Modrich, P. (1988) *J. Biol. Chem.* **263,** 6829–6835
27. Genschel, J., and Modrich, P. (2006) *Methods Enzymol.* **408,** 273–284
28. Genschel, J., Littman, S. J., Drummond, J. T., and Modrich, P. (1998) *J. Biol. Chem.* **273,** 19895–19901
29. Brown, R., Hirst, G. L., Gallagher, W. M., McIlwrath, A. J., Margison, G. P., van der Zee, A. G., and Anthoney, D. A. (1997) *Oncogene* **15,** 45–52
30. Strathdee, G., MacKean, M. J., Illand, M., and Brown, R. (1999) *Oncogene* **18,** 2335–2341
31. Guo, S., Presnell, S. R., Yuan, F., Zhang, Y., Gu, L., and Li, G. M. (2004) *J. Biol. Chem.* **279,** 16912–16917